The Conformation of H,K-ATPase Determines the Nucleoside Triphosphate (NTP) Selectivity for Active Proton Transport

William W. Reenstra, James Crothers, Jr., and John G. Forte*

Department of Molecular & Cell Biology, University of California, Berkeley, California 94720

Received May 22, 2007; Revised Manuscript Received June 27, 2007

ABSTRACT: The gastric H,K-ATPase is related to other cation transport ATPases, for example, Na,K-ATPase and Ca-ATPase, which are called E1−E2 ATPases in recognition of conformational transitions during their respective transport and catalytic cycles. Generally, these ATPases cannot utilize NTPs other than ATP for net ion transport activity. For example, under standard assay conditions, rates of NTP hydrolysis and H^+ pumping by the H,K-ATPase for CTP are about 10% of those for ATP and undetectable with GTP, ITP, and UTP. However, we observed that H,K-ATPase will catalyze NTP/ADP phosphate exchange at similar rates for all of these NTPs, suggesting that a common phosphoenzyme intermediate is formed. The present study was undertaken to evaluate the specificity of nucleotides to power the H,K-ATPase and several of its partial reactions, including NTP/ADP exchange, K^+-catalyzed phosphatase activity, and proton pumping. Results demonstrate that under conditions that promote the conformational change of the K^+ bound form of the enzyme, K·E2, to E1, all NTPs tested support K^+-stimulated NTPase activity and H^+ pumping up to 30−50% of that with ATP. These conditions include (1) the presence of ADP as well as the NTP energy source and (2) reduced K^+ concentration on the cytoplasmic side to ∼0. These data conform to structural models for E1−E2 ATPases whereby adenosine binding promotes the K·E2 to E1 conformational change and K^+ deocclusion.

Na,K-ATPase and H,K-ATPase are closely related members of a larger family of P-type, cation-transporting ATPases, which also include Ca-ATPases and several other proton transport ATPases. Na,K-ATPase and H,K-ATPase are ATP-driven cation exchange transporters sharing structural similarities, such as heterodimeric α- and β-subunits, as well as many functional similarities within their catalytic cycle (*1*−*3*). The enzymes are also called E1,E2-type ATPases in recognition of the two major conformational states where transported ions interact with the ATPase on the cytoplasmic face (E1) and the extracellular face (E2) in the catalytic cycle, modeled simply according to Scheme 1, which is the same as the Post−Albers model for the Na,K-ATPase (*3*). When a proton is bound from the cytoplasmic face, H·E1·ATP the H,K-ATPase is autophosphorylated with the transfer of the γ-phosphate from ATP to an aspartate residue (Asp387) on the α-subunit, forming the H·E1−P phosphoenzyme intermediate. A transition from the E1 to the E2 form is essential for the delivery of H^+ into the gastric luminal medium and the formation of E2−P. The binding of K^+ to the luminal face catalyzes the deposphorylation of E2−P and generates a K·E2 form of the H,K-ATPase where K^+ is tightly bound. The release of K^+ at the cytoplasmic face and formation of E1·ATP is catalyzed by the binding of ATP to K·E2. The catalytic cycle is completed by the binding of a proton at the cytoplasmic face. While Scheme 1 is sufficient for the studies present in this paper, we have shown that ATP can also bind to E2 prior to the loss of inorganic phosphate (*4*).

Scheme 1

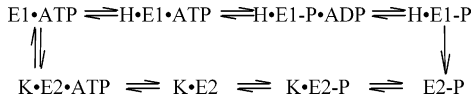

Na,K-ATPase and H,K-ATPase are generally considered to be specific, or at least very highly selective, for ATP over all other nucleotides. A number of studies have addressed the issue of nucleotide specificity for Na,K-ATPase although none have looked at H,K-ATPase in any detail. DePont's group have examined the nucleotide specificity for catalyzing the transition from K·E2 to the E1 form of the Na,K-ATPase, which they could indirectly monitor using the sensitivity of enzyme activity to trypsin as well as the fragmentation pattern of the α-subunit (*5*). From these data and earlier studies (*6*, *7*), they concluded an order of specificity, ATP > ADP > ADPNP > CTP > ITP = GTP = AMP, and that the transition from K·E2 back to E1 determined nucleotide specificity of the enzymatic cycle and coupled cation transport. For the H,K-ATPase, Sachs' group (*8*) reported that K^+-stimulated hydrolysis occurred in the sequence ATP 100, CTP 15, GTP 12, ADP 0.7, and ITP 0 (with ATP set at 100), although no details were given regarding K^+ ion or nucleotide concentrations. It was also shown that both ATP and ADP catalyzed K^+ deocclusion for the H,K-ATPase as well as the Na,K-ATPase (*9*, *10*). In a study of nucleotide metabolism by parietal cells and by H,K-ATPase-enriched membranes derived therefrom, our laboratory reported rates

* To whom correspondence should be addressed. Mailing address: Dept. of Molecular & Cell Biology, 245 LSA, MC#3200, University of California, Berkeley, California 94720. Phone: 510-642-1544. Fax: 510-643-6791. E-mail: jforte@berkeley.edu.

10.1021/bi700991n CCC: $37.00 © 2007 American Chemical Society
Published on Web 08/14/2007

for H,K-ATPase catalyzed NTP[1]/ADP exchange that were similar to the rate of ATP hydrolysis and had little nucleotide sensitivity (*11*). Given that the formation of a phosphoenzyme intermediate is essential for ATP/ADP exchange, and that the steps after E−P formation in Scheme 1 do not involve the nucleotide, there seemed to be an incongruity between the relatively nonspecific nature of nucleotides supporting NTP/ADP exchange and the high specificity for the full transport cycle. Perhaps, as predicted for Na,K-ATPase (*5*−*7*), the transition from K·E2 back to E1 determined the nucleotide specificity for H,K-ATPase.

The present study was undertaken to evaluate the specificity of nucleotides to power the H,K-ATPase and several of its partial reactions, including NTP/ADP exchange, K^+-catalyzed phosphatase activity, and proton pumping. Our findings demonstrate that under the appropriate ionic conditions at each membrane interface (i.e., K^+ concentrations), all nucleoside triphosphates tested will drive proton pumping by the H,K-ATPase. The non-adenine NTPs can substitute for ATP at all stages of the reaction cycle with the exception of binding to the K·E2 form and catalysis of K^+ deocclusion. NTP-driven proton pumping is observed when K^+ concentration on the cytoplasmic side of the membrane is very low or when ADP is present to catalyze K^+ deocclusion.

MATERIALS AND METHODS

Materials. Nucleotides and *p*-nitrophenylphosphate were purchased from Sigma Biochemicals (www.sigma-aldrich-.com). [^{14}C]-ADP was from MP Biomedicals (www.mpbio.com). Acridine orange was from Aldrich Chemicals (www.sigma-aldrich.com). All other chemicals were of the highest purity available.

Preparation of H,K-ATPase-Enriched Microsomal Vesicles. H,K-ATPase-containing microsomal vesicles were prepared from pig gastric mucosa as previously described (*12*). The fundic mucosa of pig stomach (obtained from a local slaughterhouse) was removed by scraping and rinsed in ice cold homogenization buffer (125 mM mannitol, 40 mM sucrose, 0.4 mM EDTA, 5 mM PIPES, adjusted to pH 6.7). All subsequent procedures were carried out at 0−4 °C. The mucosal scrapings were minced with scissors and homogenized with 15 passes in a Potter−Elvehjem homogenizer. The homogenate was centrifuged at 14 500 × *g* for 10 min. The supernatant was further centrifuged at 100 000 × *g* for 1 h. The resulting crude microsomal pellet was resuspended in buffer A (300 mM sucrose, 20 mM Tris-HCl, pH 7.4) and layered over a density gradient consisting of successive layers of 20%, 27%, and 33% sucrose, in 0.2 mM EDTA and 5 mM Tris-HCl, pH 7.3. After centrifugation for 2 h at 135 000 × *g*, the membrane vesicles that layered at the 20%−27% interface were harvested and stored frozen until use. Protein was determined by the method of Lowry et al. (*13*), with bovine serum albumin as the protein standard.

Hydrolysis of ATP and Other Nucleotides. H,K-ATPase activity of purified microsomal vesicles was assayed as the K^+-dependent hydrolysis of ATP. The assay was performed at 37 °C in 1 mL of medium containing 20 mM PIPES (pH 6.8), 1 mM $MgSO_4$, 1 mM ATP, and 8−15 μg of membrane protein. Separate assays were performed (i) without KCl (NaCl or choline-Cl substitution), (ii) in the presence of KCl, and (iii) in the presence of KCl and 5 μM valinomycin as a K^+ ionophore to give K^+ free access to the vesicle interior. The difference in activity with and without KCl (and valinomycin) was taken as the K^+-dependent activity. For the more general NTPase activity, other nucleotides were substituted for ATP. Test compounds were added as indicated for individual assays. The reaction was initiated by the addition of either NTP or membranes and terminated after 10 min with 1 mL of 14% trichloroacetic acid (TCA). Liberation of inorganic phosphate (P_i) was quantified by butyl acetate extraction of the phosphomolybdate complex (*14*). Activity is expressed as micromoles of P_i liberated per milligram of protein per hour.

NTP/ADP Exchange Reaction. The rate of NTP/ADP exchange catalyzed by the H,K-ATPase was measured by incubating 10−20 μg of membrane protein at room temperature in a volume of 150−200 μL containing 15 mM PIPES (pH 6.5), 1 mM $MgSO_4$, and 10 or 20 mM of either choline-Cl or KCl. A nucleotide mix, to a final concentration of 1 mM NTP, 0.1 mM ADP containing 1 μCi of [^{14}C]-ADP, was added to start the reaction. In some experiments ADP or ATP concentration was varied to determine kinetic constants. Aliquots were taken at sequential times and quenched with ice cold 20 mM EDTA. Protein was precipitated with 0.6 N perchloric acid, and the supernatants were neutralized with ice cold KOH and spotted onto polyethyleneimine−cellulose together with unlabeled nucleotide standards. Nucleotides were chromatographically separated by thin layer chromatograhy (*15*), identified by UV light, scraped from the plate, and counted by liquid scintillation to determine the fractional amount of [^{14}C]-ADP converted into [^{14}C]-NTP. The spot containing [^{14}C]-ADP was also measured. The NTP/ADP exchange rate was calculated as micromoles of ADP converted to NTP per milligram of protein per hour. Rates of nucleotide exchange were calculated only for conditions where the measured incorporation into [^{14}C]-NTP was linear in time and where the amount of [^{14}C]-AMP generated was less than 1% of the total nucleotide counts.

pH Gradient Formation by the Pump with Different K^+ Gradients. The formation of acid-interior vesicular pH gradients by the proton pump was monitored by the acridine orange (AO) uptake assay, a fluorescent weak base whose vesicular accumulation and self-quenching occur according to the pH gradient (*12*, *16*). One typical assay condition included 100 mM KCl, 10 mM *N*-methyl glucamine (NMG)−TES buffer, pH 7.0, 1 mM $MgSO_4$, 0.1 mM EGTA, 2 μM valinomycin, 4 μM acridine orange, and 10−15 μg/mL of microsomal vesicles all mixed within a spectrofluorometer cuvette. The AO uptake reaction was started by addition of NTP to the cuvette, and the fluorescence emission at 530 nm (excitation at 493 nm) was recorded. Under these initial conditions, the external (extravesicular) K^+ concentration ($[K^+]_o$) was 100 mM and intravesicular K^+ ($[K^+]_i$) was low. In other experiments, the K^+ gradient was varied by specifically elevating $[K^+]_i$ and varying the concentration of extravesicular $[K^+]_o$. For these experiments, vesicles were preincubated in 100 mM KCl, 10 mM NMG−TES buffer, pH 7.0, 1 mM $MgSO_4$, and 0.1 mM EGTA for 90 min at room temperature. The vesicles were then centrifuged at

[1] Abbreviations: NTP, nucleoside triphosphate; pNPP, paranitrophenylphosphate; AO, acridine orange; NMG-Cl, *N*-methyl glucamine chloride; PIPES, piperazine-*N*,*N*′-bis (2-ethanesulfonic acid); TES, *N*-tris (hydroxymethyl) methyl-2-aminoethanesulfonic acid.

Table 1: Basal and K^+-Stimulated NTPase Activities in the Absence and Presence of ADP for Gastric Microsomal Vesicles[a]

nucleotide	0 K^+	10 mM K^+	10 mM K^+ + val
ATP	5.84 ± 1.10 (5)	18.15 ± 3.81 (5)	37.57 ± 0.44 (3)
ATP + ADP	4.46 ± 0.75 (5)	15.55 ± 4.03 (5)	38.45 ± 0.11 (2)
CTP	6.22 ± 0.91 (3)	7.63 ± 1.26 (3)	15.25 ± 0.60 (2)
CTP + ADP	5.43 ± 0.73 (4)	8.92 ± 0.98 (4)	19.00 ± 0.57 (2)
ITP	6.69 ± 1.01 (5)	5.77 ± 0.66 (5)	6.42 ± 0.59 (3)
ITP + ADP	5.40 ± 0.55(7)	9.18 ± 0.67 (7)	17.65 ± 0.42 (4)
GTP	7.84 ± 0.31 (2)	6.24 ± 0.31 (2)	5.66 ± 0.39 (2)
GTP + ADP	5.28 ± 0.90 (3)	8.51 ± 1.43 (3)	14.37 ± 0.80 (2)
UTP	3.80 (1)	2.30 (1)	2.20 (1)
UTP + ADP	5.50 (1)	10.30 (1)	17.50 (1)

[a] Rates of H,K-ATPase activity are expressed in μmol/(mg protein h) ± SEM for measurements, where $N = 3$ or greater (indicated in parentheses). Where $N = 2$, values are expressed ± range. All nucleoside triphosphates were present at 1 mM, where indicated ADP was present at 0.1 mM. val = 3 μM valinomycin.

135 000 × *g* for 45 min in the cold and resuspended in K^+-free medium (100 mM NMG-Cl, 10 mM NMG-TES, pH 7.0, 0.1 mM EGTA) at 0 °C. For the AO uptake assay, the K^+-loaded vesicles were added to a solution of designated $[K^+]_o$ prepared by proportionally mixing solutions of 100 mM NMG-Cl and 100 mM KCl, including 10 mM NMG−TES, pH 7.0, 1 mM $MgSO_4$, 0.1 mM EGTA, and 2 μM AO. As above, the NTPs were added to start the reaction as indicated for the individual experiment.

pNPPase Activity. *p*-Nitrophenyl phosphatase (pNPPase) activity of the H,K-ATPase was assayed by measuring the K^+-dependent conversion of *p*-nitrophenylphosphate to *p*-nitrophenol. Assays were performed at 37 °C in either 1 or 3 mL volume containing 20 mM Tris-HCl (pH 7.2), 5 mM $MgSO_4$, 5 mM pNPP, with and without KCl and various test compounds, and initiated by adding 3−8 μg of membrane protein. Two methods were used to monitor the hydrolysis of pNPP. For individual "tube assays", the total volume was 1 mL, and the reactions were terminated after 10 min with 1.5 mL of 1 N NaOH. The samples were clarified by centrifugation, and the OD was measured at 410 nm. For the "spectrophotometric assay", sample volumes of 3 mL were included in optically clear cuvettes within a multiwell chamber of a Cary 210 spectrophotometer, and OD readings at 410 nm were continuously recorded as increasing concentrations of NTP inhibitors were successively added. Total added volume never exceeded 5% of the cuvette volume. The ΔOD/min, along with the extinction coefficient and protein concentration, were used to calculate pNPPase activity. For both methods, activity was expressed as micromoles of *p*-nitrophenol liberated per milligram of protein per hour.

Kinetic Analyses. Kinetic constants were calculated from Lineweaver−Burke and Dixon plots and presented as the mean ± SEM for the number of experiments (*N*) as indicated. Where applicable statistical significance was determined by comparing the mean and population variance using a *t*-test.

RESULTS

Gastric Microsomes Selectively Hydrolyze Various Nucleotides. The ability of gradient-purified gastric microsomes to hydrolyze various nucleotides (NTPs) is shown in Table 1. In the absence of K^+, all nucleotides tested supported basal NTPase activity to roughly the same extent. As is well established for gastric microsomal vesicles, basal ATPase activity was stimulated by K^+, and this was further greatly enhanced by inclusion of the K^+ ionophore valinomycin, which provides access of K^+ to intravesicular sites (*12*, *16*). CTPase activity was also stimulated by K^+ plus valinomycin, unlike ITP, GTP, and UTP, all of which tended to be slightly inhibited by 10 mM K^+. Addition of 0.1 mM ADP had no significant effect on ATPase activity ($P > 0.05$), with or without K^+. Surprisingly, however, ADP induced an increase in K^+-stimulated hydrolysis for all other nucleotides tested (except for ATP) and a significant increase in activity in the presence of K^+ and valinomycin.

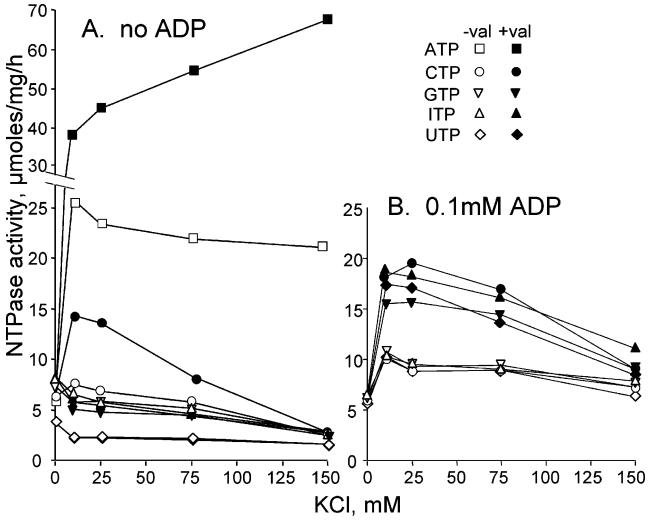

FIGURE 1: Hydrolysis of NTPs by H,K-ATPase in the presence and absence of ADP is variably affected by K^+ concentration. Gastric microsomal vesicles were incubated with 1 mM NTP and at various K^+ concentrations as indicated, in the absence (open symbols) or presence (closed symbols) of 2 μM valinomycin: (A) NTP hydrolysis with no ADP present; (B) NTP hydrolysis in the presence of 0.1 mM ADP.

The effects of a full range of K^+ concentrations on NTPase, both with and without valinomycin, are shown in Figure 1A. ATPase activity is highly dependent upon K^+ concentration and valinomycin. In the absence of the K^+ ionophore, ATPase was maximal at approximately 10 mM K^+ and tended to decrease at higher concentrations, whereas in the presence of valinomycin ATPase activity increased with higher K^+ concentration, although the dependence on K^+ concentration was much greater from 0 to 10 mM K^+ than from 10 to 150 mM. At 150 mM K^+ plus valinomycin, the K^+-stimulated ATPase activity was 12 times higher than basal rate. As noted in Table 1, in the absence of ADP, CTP was the only other nucleotide for which we observed any K^+-stimulated hydrolysis, but unlike ATPase, the CTPase activity was inhibited by high concentrations of K^+ even in the presence of valinomycin. The ITPase, GTPase, and UTPase activities were all inhibited by K^+. In the presence of ADP (Figure 1B), the hydrolysis of ITP, GTP, and UTP was increased in the range of 10−20 mM K^+, with a further enhancement by valinomycin, but inhibited by higher K^+ concentrations. We conclude that there is relatively little NTP selectivity for the basal (0 K^+) rates of hydrolysis by gastric microsomes, but there is high selectivity for K^+-stimulated NTPase activity: ATP ≫ CTP > other NTPs, especially at physiological levels of cytoplasmic K^+ and under conditions that increase luminal K^+ concentration. The situation changes

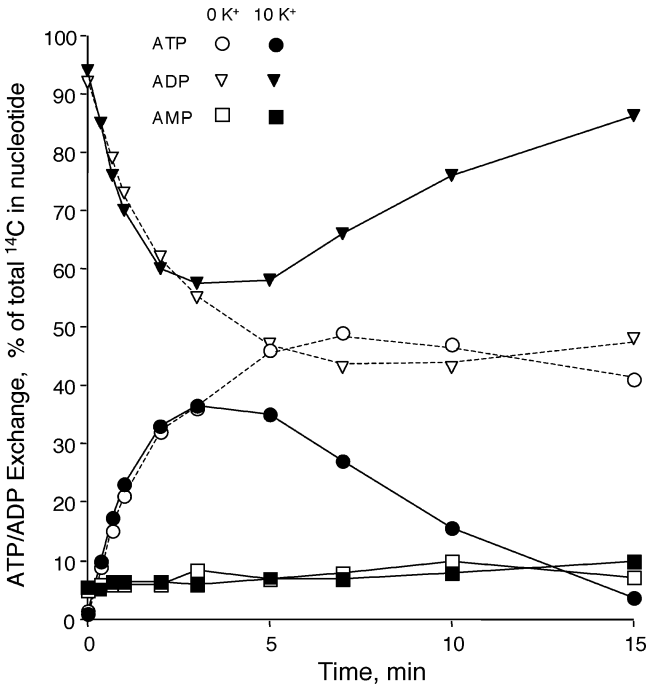

FIGURE 2: Time course of ATP/ADP phosphate exchange reaction. Gastric microsomal vesicles were incubated with 0.1 mM [^{14}C]-ADP and 1.0 mM ATP at 37 °C, in the presence of either 10 mM NaCl (0 K^+) or 10 mM KCl (+K^+). Aliquots were taken at various times, and the reaction was stopped and protein removed as described in Materials and Methods. Labeled nucleotides in the supernatants were separated by TLC and designated spots were cut out and counted for percent of total ^{14}C incorporated into ATP, ADP, or AMP at each time point. Within the first 1−2 min, the increase in ^{14}C incorporation into ATP was linear and equivalent to the loss of ^{14}C from ADP, with very little dependence on K^+. With longer times, there was obvious bending of the curves due to (i) exchange equilibration of the label between ADP and ATP and (ii) steady hydrolysis and conversion of ATP into ADP, the latter being accelerated in the presence of K^+. Negligible label was incorporated into AMP over the entire 15 min time course indicating very little hydrolysis of ADP or conversion of 2ADP to ATP + AMP.

when ADP is included in the mix; then all NTPases except ATPase are activated by K^+, although the rate of ATPase (Table 1) is greater than that of the non-adenine nucleotides, and the latter are still inhibited by high K^+ concentration (Figure 1B).

Gastric Microsomes Promote a High Rate of ADP/NTP Exchange for All Nucleotides. NTP/ADP exchange is a well described partial reaction of Na,K-ATPase and H,K-ATPase (*11*, *17*). The ATP/ADP exchange activity of gastric microsomes is shown in Figure 2. In the absence of K^+, ADP rapidly accepts phosphate from ATP and the ^{14}C label nearly equilibrates between ATP and ADP over the 15 min time course. Hydrolysis of ADP to AMP is extremely low. In the presence of K^+, the initial rates (within the first 1−2 min) are nearly the same as those in the absence of K^+. However, at later times, the ^{14}C label is reincorporated back into the ADP pool as ATP is hydrolyzed. Again, hydrolysis of ADP to AMP is trivial. The principal effect of K^+ in these studies was an increase in the rate of ATP hydrolysis, with little change in the rate of ATP/ADP exchange. These data demonstrate an ATP/ADP exchange activity in gastric microsomes with rates comparable to those of K^+-stimulated ATP hydrolysis consistent with earlier reports (*11*, *17*). However, it is clear from Figure 2 that the rate of ATP/ADP exchange must be measured at early times (<2 min) when the other enzymatic activities of the microsomes do not alter the initial rate conditions. Additional experiments (data not shown) revealed several other characteristics for ATP/ADP exchange: at 1.25 mM ATP and 1 mM Mg^{2+}, the K_m for ADP is ~100 μM; ATP/ADP exchange activity is inhibited by 0 Mg^{2+} (EDTA) or by *p*-chloromercuribenzenesulfonate, and ATP/ADP exchange is not sensitive to K^+-competitive inhibitors of H,K-ATPase (e.g., SCH28080).

Table 2: Rate of [^{14}C]-ADP/NTP Exchange for Various Nucleotides[a]

nucleotide	0 K^+	10 mM K^+
ATP	18.4 ± 1.0 (8)	19.1 ± 1.1 (6)
CTP	8.9 ± 1.3 (6)	8.6 ± 2.4 (4)
GTP	7.0 ± 1.3 (4)	4.9 ± 2.5 (2)
ITP	13.5 ± 2.0 (6)	11.1 ± 2.7 (3)
UTP	9.3 ± 3.0 (2)	6.8 ± 1.1 (2)

[a] Reaction was started by adding gastric microsomes to the nucleotide ([^{14}C]-ADP/NTP) mix, and samples were taken for ^{14}C incorporation into nucleotide triphosphates at successive time intervals; the rate of exchange was calculated for samples taken over the first 2 min of reaction time. Rates of exchange are given as μmol/(mg protein h) ± SEM for *N* preparations (parentheses). In cases where only two measurements were made, values are given ± range. ADP concentration was 0.1 mM in all cases; nucleoside triphosphate concentration was either 1 or 1.25 mM.

The rates of ADP/NTP exchange for a variety of nucleoside triphosphates, with and without 10 mM K^+, are shown in Table 2. Gastric microsomes clearly catalyze a high rate of phosphate exchange between all nucleoside triphosphates and ADP. Although the exchange rates for all nucleotides tested are within a factor of 3, the rate for ATP was significantly greater than that for the other nucleoside triphosphates. Addition of 10 mM K^+ had no significant effect on the exchange rate for any nucleotide.

Effects of Nucleotides on the K^+-Stimulated Phosphatase Activity of the H,K-ATPase. Another exchange reaction of the H,K-ATPase is incorporation of [^{18}O]H_2O into inorganic phosphate. The reaction is highly dependent upon K^+ and involves the formation and subsequent hydrolysis of a phosphoenzyme intermediate. The K^+-stimulated hydrolysis of substrates, such as acetyl phosphate and *p*-nitrophenylphosphate (pNPP), is often used to model this reaction. Here we examined the influence of various nucleotides on the K^+-stimulated *p*-nitrophenylphosphatase activity (K^+-pNPPase). Under our standard conditions (10 mM K^+), relatively low concentrations of ATP inhibit K^+-pNPPase by a noncompetitive mechanism and with a K_i^{ATP} of 5.3 ± 0.3 μM. (Figure 3A,B). The K_i for inhibition by ATP was dependent upon the K^+ concentration, and increased from 2.8 to 22 μM ATP as K^+ concentration was increased from 2 to 100 mM (data not shown). It is of interest that when the kinetic data were examined over a broader range of ATP concentration, there was a distinct break in the Dixon plot of 1/*V* vs ATP concentration (inset to Figure 3B) and at concentrations >10 μM K^+ a second K_i of 27 ± 4 μM was observed. Such a break in the Dixon plot is indicative of multiple mechanisms for ATP-dependent inhibition and, as discussed later, highlights several critical features of the H,K-ATPase catalytic cycle.

The data obtained for ATP can be contrasted with those obtained for other nucleotides as summarized in Table 3.

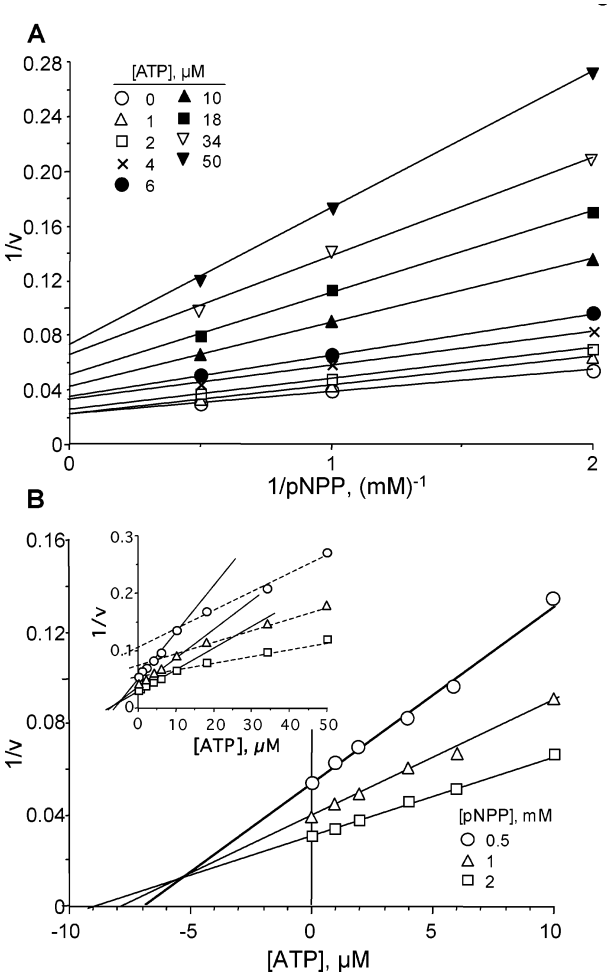

FIGURE 3: ATP effectively inhibits K^+-stimulated phosphatase activity of gastric H,K-ATPase-rich vesicles. K^+ stimulated hydrolysis of pNPP, v in μmol/(mg protein min), was measured as described in Materials and Methods under conditions where both substrate and ATP, as an inhibitor, were varied: (A) data plotted according to Lineweaver−Burke demonstrating that inhibition by ATP is not competitive (no common intercept on $1/v$ axis); (B) Dixon plot showing linear inhibition kinetics at low ATP concentrations (<10 μM ATP) with an apparent K_i of about 5 μM ATP. The inset shows a much higher range of ATP demonstrating a distinct bend in the inhibitor plot above 10 μM ATP.

Table 3: Kinetic Properties for Inhibition of pNPP Hydrolysis[a]

	type of inhibition	Dixon plot	low K_i	high K_i	N
ATP	mixed	nonlinear	5.3 ± 0.3	27 ± 4	7
CTP	mixed	nonlinear	80 ± 10	350 ± 60	3
GTP	competitive	linear		300	1
ITP	competitive	linear		400	1
ADP	mixed	linear		200 ± 30	7
Pi	competitive	linear		700 ± 100	3

[a] All values are expressed in μM. Where applicable SEMs and the number of independent measurements are given.

First, all the other nucleotides tested had estimated K_i values much higher than ATP, for example, 200 μM or greater. Second, three patterns of inhibition were observed. GTP, ITP, and inorganic phosphate appeared to be simply competitive with pNPP for hydrolysis. CTP showed an inhibition pattern similar to that for ATP although the high and low K_i's were much greater (Table 3) and the magnitude of pNPPase inhibition at low CTP concentrations was much less (data not shown) than that observed with ATP. Last, ADP, like

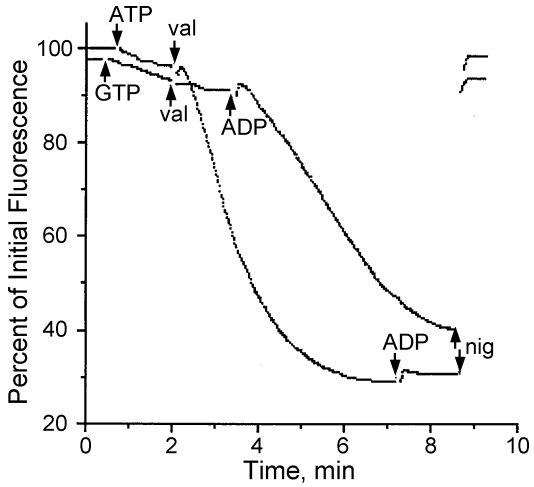

FIGURE 4: NTP-mediated H^+ transport by is promoted by ADP. Proton uptake by gastric microsomal vesicles was measured by acridine orange (AO) fluorescence quenching as described in Materials and Methods. In this experiment, vesicles were incubated in solution containing 75 mM KCl, 1 mM $MgSO_4$, 10 mM *N*-methyl glucamine−TES buffer (pH 7.0), and 4 μM AO, arbitrarily set to 100% fluorescence. Addition of 1 mM ATP or 1 mM GTP initially had very little effect in either case, but the subsequent addition of 2 μM valinomycin (val) to ATP promoted rapid quenching of AO indicating effective vesicular proton uptake as K^+ gained access to intravesicular activating sites. Valinomycin itself induced no change in the case of GTP; however, the subsequent addition of 0.1 mM ADP produced effective proton uptake. Finally, the addition of 2 μM nigericin (nig), a K^+/H^+ exchange ionophore, caused immediate dissipation of the ATP and GTP generated proton gradients.

ATP, displayed kinetics of mixed inhibition; however, the observed K_i^{ADP} was significantly greater than that for ATP, and the Dixon plots were linear. The mixed kinetics as seen with ATP, CTP, and ADP are a reflection of their ability to bind to an ATP binding site when the K^+ and phosphate sites are occupied. Nucleotides such as GTP and ITP that only show competitive kinetics are thought to bind solely to the phosphate binding site in competition with pNPP or phosphate.

Dependence of Proton Transport on Nucleotides. The ability of various nucleotides to support proton transport by gastric microsomal vesicles was assayed by acridine orange uptake under conditions with varying K^+ gradients. When freshly isolated vesicles (zero intravesicular K^+) were incubated in a medium of 150 mM K^+, only ATP was capable of driving proton transport into the vesicles as demonstrated in Figure 4. Moreover, this occurred only after valinomycin was included in order to allow K^+ to enter the vesicles and support the H^+/K^+ exchange activity of the pump in keeping with the pump/leak model of gastric microsomes (*16*, *18*). As shown for GTP in Figure 4, all other NTPs were incapable of driving vesicular proton uptake under these conditions where extravesicular K^+ was high (data not shown). However, consistent with what we observed for NTPase activities, these other NTPs would support proton uptake if ADP was added to the medium (Figure 4). Since ADP alone did not support proton transport, this suggested that either the NTP/ADP exchange reaction or the adenine moiety from ADP played a critical role in the transport cycle. These transport data are also reminiscent of the H,K-ATPase activities where NTP plus ADP, in the presence of 10 mM K^+ and valinomycin, supported turnover

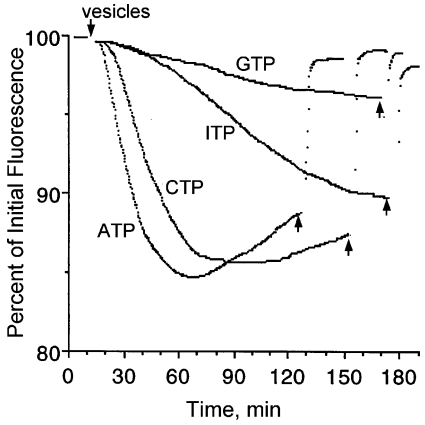

FIGURE 5: NTP-mediated H^+ transport when $[K^+]_o$ is low and $[K^+]_i$ is high. Proton uptake by gastric microsomal vesicles was measured by acridine orange (AO) quenching. Microsomes were first incubated in 100 mM KCl containing 10 mM *N*-methyl glucamine−TES buffer (pH 7.0), 1 mM $MgSO_4$, 0.1 mM EGTA at 25 °C for 90 min. Microsomes were then diluted 50-fold into K^+-free 100 mM *N*-methylglucamine-Cl solutions containing 1 mM $MgSO_4$, 4 μM AO, and 1 mM various NTP as indicated on the recording. Under these conditions with 2 mM KCl in the extravesicular (cytoplasmic) medium and considerably higher (but unknown) K^+ within the vesicles, all NTPs tested promoted significant rates of proton uptake, with the preference ATP > CTP > ITP > GTP.

of the catalytic cycle to rates approximately one-third that of ATP (cf. Table 1).

Because the H,K-ATPase-catalyzed NTPase activity of most NTPs was clearly inhibited by high extravesicular K^+ concentration (Table 1; Figure 1), we set up conditions where K^+ was present within the vesicles but not outside the vesicles. When gastric vesicles were preloaded with KCl and diluted into a K^+-free medium such that extravesicular K^+ was reduced to ~2 mM, all nucleotides supported proton uptake to some degree with a selectivity of ATP > CTP > ITP > GTP (Figure 5). Proton uptake was independent of valinomycin and required conditions where intravesicular K^+ concentration was high and extravesicular K^+ concentration was low. Effective proton uptake by NTPs in K^+ preloaded vesicles where extravesicular K^+ concentration was very low (<1 mM) is shown in Figure 6. It is also clear from these data that, in contrast to ATP, as the extravesicular K^+ concentration was increased, CTP-, ITP-, and GTP-dependent (latter not shown) proton transport activities were all reduced (Figure 6). These proton transport data are consistent with the hydrolysis and exchange data given above and demonstrate that nucleotides other than ATP can power the gastric proton pump. However, under physiological concentrations of K^+ and ADP, only ATP is able to drive the cyclic turnover of the enzyme.

DISCUSSION

Selectivity of NTPs. In this study, we have examined several biochemical reactions and partial reactions of the gastric H,K-ATPase with special reference to the selectivity of the enzyme for various nucleoside triphosphates (NTPs). When measured at relatively low K^+ concentration, 10 mM, the K^+-stimulated hydrolytic activity showed the same preference for NTPs as reported by Sachs' group (*1*), with ATP ≫ CTP and the other NTPs having virtually no activity. Surprisingly, when the reaction medium included ADP, all NTPs had significant K^+-stimulated rates, albeit ATP was the preferred substrate. The stimulatory effect of ADP was clearly not due to hydrolysis of ADP per se because the rate of ADP → AMP + P_i was negligible (cf. Figure 2). These NTPase data, along with the measured high rates of NTP/ADP exchange, led us to postulate that the nucleotide binding and phosphoenzyme (E−P) formation could operate at relatively equivalent rates for all NTPs if the enzyme were converted from the K^+-occluded K·E2 form to the E1 form. Observations consistent with this thesis were suggested for Na,K-ATPase, where in the absence of K^+ (but presence of Na^+) the levels of phosphoenzyme formed and rates of hydrolysis were roughly equivalent for ATP, CTP, or GTP (*7*, *19*). Since the hydrolysis of CTP or GTP was diminished in the presence of K^+, as compared with ATP, the authors

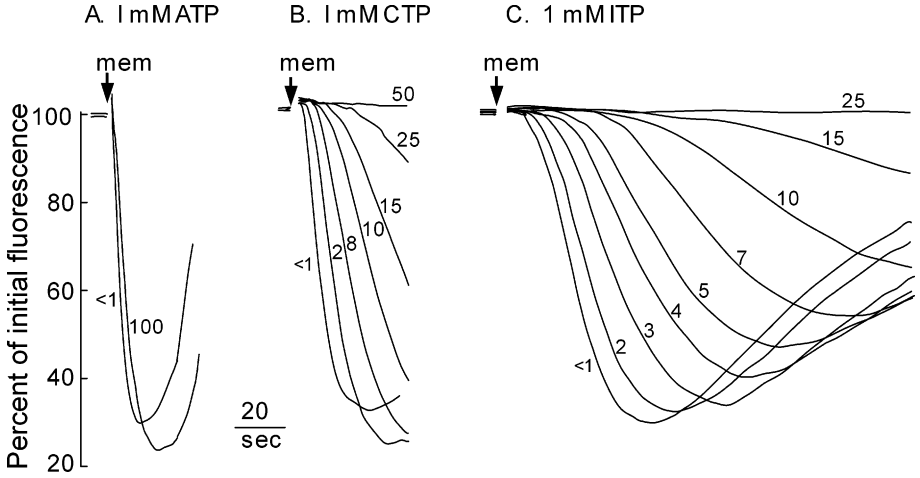

FIGURE 6: The effect of increasing extravesicular (cytoplasmic) K^+ on vesicular proton uptake mediated by ATP, CTP, or ITP. Microsomal vesicles were first incubated in 100 mM KCl containing 10 mM *N*-methyl glucamine (NMG)−TES buffer (pH 7.0), 1 mM $MgSO_4$, 0.1 mM EGTA at 25 °C for 90 min then centrifuged at 45 000 rpm for 30 min. The microsomal pellet was then resuspended in ice cold K^+-free 100 mM NMG-Cl solutions containing 10 mM NMG−TES buffer (pH 7.0), 1 mM $MgSO_4$ and 0.1 mM EGTA. This concentrated stock of microsomes were then diluted 50-fold into cuvettes containing 1 mM $MgSO_4$, 4 μM AO, and mixtures of 100 mM NMG-Cl/100 mM KCl to provide various concentrations of K^+ as indicated. The solutions also included 1 mM of either ATP (A), CTP (B), or (C) ITP as indicated, and the quenching of AO signal was followed. Under conditions when extravesicular medium contained less than 1 mM K^+, all three nucleotides supported vigorous rates of proton uptake with ATP > CTP > ITP. For both CTP and ITP, proton uptake was extremely sensitive to increase in extravesicular K^+, whereas ATP showed relatively small effects, even going to 100 mM K^+.

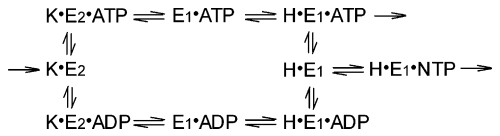

FIGURE 7: Scheme to account for nucleotide interaction with the H,K-ATPase. On the left, ATP or ADP binds with the adenosine binding site of the K^+ occluded form of the enzyme (K·E2) promoting the loss of K^+ to the cytoplasm and conformational change to the E1 form, which is stabilized by the binding of protons. In the H·E1 state, other NTPs can exchange with ADP, and the resulting H·E1·NTP complex forms the phosphoenzyme intermediate.

concluded that the non-adenine NTPs were unable to promote the K·E2 → E1 + K^+ transition for the Na,K-ATPase. We observed the same results and reached the same conclusions for the gastric H,K-ATPase. Analogous data were obtained for the Ca-ATPase of sarcoplasmic reticulum from skeletal muscle, whereby roughly equivalent maximum levels of Ca^{2+}-dependent E−P were formed from ATP, ITP, or GTP (*20*). However, ATP was much more efficient than the other NTPs in driving the full catalytic turnover involving Ca^{2+} transport (*20*−*22*). Thus the high degree of selectivity for ATP in these P-type ATPases is related to the E2 conformer state, which can be minimized by the reaction ATP + K·E2 → E1·ATP + K^+.

NTP/ADP Exchange Reaction and Proton Transport. For the H,K-ATPase, all NTPs tested here participate in phosphate exchange with ADP; rates of NTP/ADP exchange differ by less than 3-fold and show little influence of added K^+. The exchange reaction demonstrates that all NTPs are able to phosphorylate the H,K-ATPase in the presence of ADP. A similar conclusion can be reached from the observation that NTPs can drive K^+-dependent proton transport in the presence of ADP. In the absence of ADP, extravesicular (cytoplasmic) K^+ prevents proton transport by NTPs other than ATP, most likely by competing with the binding of NTPs to an E1 form of the ATPase. However if extravesicular K^+ is low, intravesicular K^+ can facilitate NTP-dependent proton transport in the absence of added ADP. When viewed in terms of the model in Scheme 1, these observations raise the following conundrum. If NTPs can phosphorylate the ATPase in the presence of extravesicular K^+, what prevents proton transport under conditions where ATP would normally support transport? Conversely, if extravesicular K^+ prevents phosphorylation of the ATPase by NTPs, how does the addition of ADP allow phosphorylation and net proton transport to occur? The most likely explanation is that ADP acts as an ATP congener. This scheme is presented in Figure 7 where three pathways for the conversion of K·E2 to H·E1 are shown. One involves the ATP-dependent deocclusion of K^+ that occurs in the presence of ATP. The second is a nucleotide-independent pathway that generates H·E1, which can bind NTP; this occurs in the absence of adenosine nucleotides when extravesicular K^+ is low. The third is the postulated ADP-dependent pathway. ADP facilitates the deocclusion of K^+ by binding to K·E2, leading to formation of E1 and the binding of an extravesicular proton. If binding of a proton at the extravesicular (cytoplasmic) surface of the ATPase (H·E1) prevents K^+ binding to E1, then the loss of ADP and binding of NTP can proceed to phosphorylation without inhibition by extravesicular K^+. This would also be consistent with the observation that in the presence of K^+, ADP stimulates the NTPase activity and proton transport generated by CTP, GTP, ITP, and UTP.

ADP-Stimulated Reaction Data from Other Studies. Experimental evidence for ADP binding to K·E2 can also be inferred from studies of the rate of K^+ deocclusion. For the H,K-ATPase and Na,K-ATPase, the deocclusion of K^+ has been shown to be effectively catalyzed by both ATP and ADP (*9*, *10*). This explanation for the effects of ADP is also consistent with recent structural studies of the Ca-ATPase and the Na,K-ATPase. For the Ca-ATPase of sarcoplasmic reticulum (SERCAa1), ATP has been shown to bind to an E2 form of the enzyme in which the adenosine binding site is distant from the phosphorylation site (*23*−*27*). In addition, ATP binding appears to induce a conformational change that generates a site for Ca^{2+} binding and positions the γ-phosphate near the site of ATP phosphorylation, Asp351. As also demonstrated by kinetic data (*28*), the structural studies suggest that Ca^{2+} binding is required before phosphorylation can proceed. Structural studies on the ATP binding domain of the Na,K-ATPase (*29*) suggest that (1) when ATP is bound the adenosine binding domain has minimal interactions (*29*) with the γ-phosphate of ATP, and (2) ATP- and ADP-dependent conformational changes are likely to be associated with K^+ deocclusion. For the H,K-ATPase, these results are consistent with ATP or ADP binding to a K·E2 form of the enzyme to facilitate K^+ deocclusion, convert E2 to E1, and generate a site for proton binding on the cytoplasmic side. In addition, if the loss of ADP from E1 is facile, NTP binding, hydrolysis, and proton transport could all be promoted by ADP. We propose that in the presence of cytoplasmic K^+, the non-adenine NTPs are virtually incapable of binding to the adenosine binding pocket and driving K·E2 to E1·NTP + K^+, but that they do form a functional E1·NTP complex once ADP has catalyzed the K·E2 to E1 conversion. The resulting E1−P·NDP product can then go "forward" to the productive transport cycle or "reverse" to produce ATP from NDP/ADP exchange, as predicted by Figure 7.

Inhibition of pNPPase Activity by NTPs. The K^+-stimulated pNPPase is thought to involve pNPP binding to K·E2, the formation of K·E2−P, and its subsequent hydrolysis via some of the same reactions that occur during ATP hydrolysis. The data presented here are consistent with all NTPs being able to bind to the K·E2 form of the enzyme via the γ-phosphate and thereby competitively inhibit hydrolysis of pNPP with low affinity. This interaction is not the same as that described for the interaction of ADP and ATP with the nucleotide binding site, and it does not promote the K·E2 to E1 conversion. On the other hand, ATP (and to a small extent CTP) is able to inhibit pNPP hydrolysis by binding to the adenosine site and form K·E2·pNPP·ATP and K·E2·ATP complexes with rapid conversion to the E1·ATP form. Inhibition by this mechanism will be noncompetitive with pNPP and reduced by elevated concentrations of K^+ as observed. However, since bound ATP is also hydrolyzed by the mechanism shown in Scheme 1, there will always be a finite amount of K·E2 product present, even at saturating levels of ATP. This mechanism suggests that at saturating ATP concentrations there should be a finite, nonzero rate of pNPP hydrolysis. Since ATP can also bind to K·E2 via the γ-phosphate, as postulated for the other NTPs, an additional

competitive inhibitory phase as observed at high ATP concentrations should occur.

Homology modeling, based on the Ca-ATPase structures, has been used to develop models for the Na,K-ATPase (*29*) and H,K-ATPase (*30*−*32*). Both modeling and mutational studies suggest that the K^+ binding pocket of H,K-ATPase includes three glutamate residues and one lysine, E343, E795, E820, and K791 (*32*−*34*). However, substitution of E820 with glutamine produced a mutant, E820Q, that displays a preference for the E1 conformation, whereas wild-type H,K-ATPase displays a preference for the E2 conformation. Since the primary deficit of non-adenine NTPs is the inability to promote the E2 → E1 transition, it will be of interest to examine NTP-driven proton transport and the effects of extravesicular K^+ for the E820Q mutant.

Conclusions. This study supports the dual roles for ATP in the transport cycle of the gastric H,K-ATPase, and by inference the Na,K- and Ca-ATPases. In addition to its role in phosphorylating the ATPase, the adenosine moiety binds specifically to the K·E2 form of the ATPase to facilitate the loss (deocclusion) of bound K^+. These two roles for ATP were clearly revealed by the differences in activities of ATP and other NTPs. While NTPs other than ATP were able to drive net H^+ transport, they were only able to do this when experimental conditions favored the deocclusion of K^+, that is, the removal of extravesicular K^+ or the presence of ADP, which shares the deocclusion role of ATP.

REFERENCES

1. Sachs, G. (1977) H+ transport by a non-electrogenic gastric ATPase as a model for acid secretion, *Rev. Physiol. Biochem. Pharmacol. 79*, 133−162.
2. Chow, D. C., and Forte, J. G. (1995) Functional significance of the beta-subunit for heterodimeric P-type ATPases, *J. Exp. Biol. 198*, 1−17.
3. Jorgensen, P. L., Hakansson, K. O., and Karlish, S. J. (2003) Structure and mechanism of Na,K-ATPase: functional sites and their interactions, *Annu. Rev. Physiol. 65*, 817−849.
4. Reenstra, W. W., Bettencourt, J. D., and Forte, J. G. (1988) Kinetic studies of the gastric H,K-ATPase. Evidence for simultaneous binding of ATP and inorganic phosphate, *J. Biol. Chem. 263*, 19618−19625.
5. Schuurmans Stekhoven, F. M., Swarts, H. G., Zhao, R. S., and de Pont, J. J. (1986) Nucleotide specificity of the E2K−-E1K transition in (Na+ + K+)-ATPase as probed with tryptic inactivation and fragmentation, *Biochim. Biophys. Acta 861*, 259−266.
6. Robinson, J. D. (1982) Differences between CTP and ATP as substrates for the (Na + K)-ATPase, *Arch. Biochem. Biophys. 213*, 650−657.
7. Fu, Y. F., Schuurmans, Stekhoven, F. M., Swarts, H. G., de Pont, J. J., and Bonting, S. L. (1985) The locus of nucleotide specificity in the reaction mechanism of (Na+ + K+)-ATPase determined with ATP and GTP as substrates, *Biochim. Biophys. Acta 817*, 7−16.
8. Sachs, G., Chang, H. H., Rabon, E., Schackman, R., Lewin, M., and Saccomani, G. (1976) A nonelectrogenic H+ pump in plasma membranes of hog stomach, *J. Biol. Chem. 251*, 7690−7698.
9. Glynn, I. M., and Richards, D. E. (1982) Occlusion of rubidium ions by the sodium-potassium pump: its implications for the mechanism of potassium transport, *J. Physiol. 330*, 17−43.
10. Rabon, E. C., Smillie, K., Seru, V., and Rabon, R. (1993) Rubidium occlusion within tryptic peptides of the H,K-ATPase, *J. Biol. Chem. 268*, 8012−8018.
11. Rong, Q., Utevskaya, O., Ramilo, M., Chow, D. C., and Forte, J. G. (1998) Nucleotide metabolism by gastric glands and H(+)-K(+)-ATPase-enriched membranes, *Am. J. Physiol. 274*, G103−G110.
12. Reenstra, W. W., and Forte, J. G. (1990) Isolation of H+,K(+)-ATPase-containing membranes from the gastric oxyntic cell, *Methods Enzymol. 192*, 151−165.
13. Lowry, O. H., Rosebrough, N. J., Farr, A. L., and Randall, R. J. (1951) Protein measurement with the Folin phenol reagent *J. Biol. Chem. 193*, 265−275.
14. Sanui, H. (1974) Measurement of inorganic orthophosphate in biological materials, *Anal. Biochem. 60*, 489−504.
15. Gonzales, L. W., and Geel, S. E. (1975) Thin-layer chromatography of brain adenine nucleoside and nucleotides and determination of ATP specific activity, *Anal. Biochem. 63*, 400−413.
16. Lee, H. C., and Forte, J. G. (1978) A study of H+ transport in gastric microsomal vesicles using fluorescent probes, *Biochim. Biophys. Acta 508*, 339−356.
17. Rabon, E., Sachs, G., Mardh, S., and Wallmark, B. (1982) ATP/ADP exchange activity of gastric (H+ +K+)-ATPase, *Biochim. Biophys. Acta 688*, 515−524.
18. Lee, H. C., Breitbart, H., Berman, M., and Forte, J. G. (1979) Potassium-stimulated ATPase activity and hydrogen transport in gastric microsomal vesicles, *Biochim. Biophys. Acta 553*, 107−131.
19. Guerra, M., Robinson, J. D., and Steinberg, M. (1990) Differential effects of substrates on three transport modes of the Na+/K(+)-ATPase, *Biochim. Biophys. Acta 1023*, 73−80.
20. de Meis, L., and Fialho de Mello, M. C. (1973) Substrate regulation of membrane phosphorylation and of Ca 2+ transport in the sarcoplasmic reticulum, *J. Biol. Chem. 248*, 3691−3701.
21. Galina, A., and de Meis, L. (1991) Ca2+ translocation and catalytic activity of the sarcoplasmic reticulum ATPase. Modulation by ATP, Ca2+, and Pi, *J. Biol. Chem. 266*, 17978−17982.
22. Worsfold, M., and Peter, J. B. (1970) Kinetics of calcium transport by fragmented sarcoplasmic reticulum, *J. Biol. Chem. 245*, 5545−5552.
23. Toyoshima, C., Nakasako, M., Nomura, H., and Ogawa, H. (2000) Crystal structure of the calcium pump of sarcoplasmic reticulum at 2.6 A resolution, *Nature 405*, 647−655.
24. Toyoshima, C., and Nomura, H. (2002) Structural changes in the calcium pump accompanying the dissociation of calcium, *Nature 418*, 605−611.
25. Toyoshima, C., and Mizutani, T. (2004) Crystal structure of the calcium pump with a bound ATP analogue, *Nature 430*, 529−535.
26. Toyoshima, C., and Inesi, G. (2004) Structural basis of ion pumping by Ca2+-ATPase of the sarcoplasmic reticulum, *Annu. Rev. Biochem. 73*, 269−292.
27. Toyoshima, C., Nomura, H., and Tsuda, T. (2004) Lumenal gating mechanism revealed in calcium pump crystal structures with phosphate analogues, *Nature 432*, 361−368.
28. Pickart, C. M., and Jencks, W. P. (1984) Energetics of the calcium-transporting ATPase, *J. Biol. Chem. 259*, 1629−1643.
29. Hilge, M., Siegal, G., Vuister, G. W., Guntert, P., Gloor, S. M., and Abrahams, J. P. (2003) ATP-induced conformational changes of the nucleotide-binding domain of Na,K-ATPase, *Nat. Struct. Biol. 10*, 468−474.
30. Koenderink, J. B., Swarts, H. G., Willems, P. H., Krieger, E., and De, Pont, J. J. (2004) A conformation-specific interhelical salt bridge in the K+ binding site of gastric H,K-ATPase, *J. Biol. Chem. 279*, 16417−16424.
31. Munson, K., Garcia, R., and Sachs, G. (2005) Inhibitor and ion binding sites on the gastric H,K-ATPase, *Biochemistry 44*, 5267−5284.
32. Vagin, O., Munson, K., Lambrecht, N., Karlish, S. J., and Sachs, G. (2001) Mutational analysis of the K+-competitive inhibitor site of gastric H,K-ATPase, *Biochemistry 40*, 7480−7490.
33. Asano, S., Tega, Y., Konishi, K., Fujioka, M., and Takeguchi, N. (1996) Functional expression of gastric H+,K(+)-ATPase and site-directed mutagenesis of the putative cation binding site and catalytic center, *J. Biol. Chem. 271*, 2740−2745.
34. Swarts, H. G., Hermsen, H. P., Koenderink, J. B., Willems, P. H., and de Pont, J. J. (1999) Conformation-dependent inhibition of gastric H+,K+-ATPase by SCH 28080 emonstrated by mutagenesis of glutamic acid 820, *Mol. Pharmacol. 55*, 541−547.

BI700991N